J|A|C|S COMMUNICATIONS

Published on Web 09/29/2009

Facile High-Yield Solvothermal Deposition of Inorganic Nanostructures on Zeolite Crystals for Mixed Matrix Membrane Fabrication

Tae-Hyun Bae, Junqiang Liu, Jong Suk Lee,
William J. Koros, Christopher W. Jones,* and Sankar Nair*

School of Chemical & Biomolecular Engineering, Georgia Institute of Technology, 311 Ferst Drive, Atlanta, Georgia, 30332-0100

Received September 2, 2009; E-mail: cjones@chbe.gatech.edu; sankar.nair@chbe.gatech.edu

Separation membranes with high performance can potentially be made by incorporating zeolites (or other nanoporous molecular sieves) in polymeric membranes. Such 'mixed matrix' membranes combine the processability and mechanical stability of polymers with the molecular sieving function of zeolites.[1] However, preparation of high-quality mixed matrix membranes has been hampered by poor adhesion between the inorganic crystals and the polymer and by inadequate dispersion of the inorganic particles. Well-known compatibilization approaches such as organic functionalization of zeolites with silane coupling agents[2] have led to poor membrane permeability[2a,d] and/or selectivity,[2b] which have been attributed to the rigidification of polymer chains at the interface. Furthermore, the use of coupling agents is usually limited to specific polymer/zeolite pairs. In a different approach, Shu et al. reported that a $Mg(OH)_2$ whisker-like nanostructured surface could be created on the surface of zeolite A via a halide/Grignard route.[3] This highly roughened surface provided enhanced polymer/zeolite adhesion via the adsorption and presumed entanglement of polymer chains in the whisker structure and yielded mixed matrix membranes with significantly improved separation performance. However, the halide/Grignard method utilizes a complicated procedure and sensitive reactants. To enable a large-scale impact of mixed matrix membranes, it is important to develop rational methods to create such nanostructures on molecular sieve surfaces, using more benign chemistry that is amenable to scale-up. Several studies demonstrate synthesis of $Mg(OH)_2$ particles in solution by precipitation,[4] hydrothermal,[5] or solvothermal processes.[6] Here we report a facile, more general, high-yield, and inexpensive solvothermal process for controlled deposition of $Mg(OH)_2$ nanostructures on a pure-silica zeolite. The permeation characteristics of mixed matrix membranes fabricated using the surface-modified materials transcend the upper bounds on polymeric membrane performance.

Pure-silica zeolite MFI crystals of different sizes (5 μm, 2 μm, 300 nm, and 100 nm) were synthesized hydrothermally (Figure S1). Solvothermal deposition of $Mg(OH)_2$ was performed at 160 °C in a solvent mixture of ethylenediamine and a $MgSO_4$ aqueous solution. For control studies, surface treatments were also performed using the Grignard route after seeding the zeolite surfaces with NaCl.[7] Figure 1 shows the morphology of the MFI crystals after solvothermal deposition. Well-defined whiskers with high surface density formed on 2 and 5 μm MFI crystals, which provide a large planar surface for nanocrystal nucleation and growth and/or deposition. The morphology of the solids deposited on the 300 nm MFI particles was different, and the particles had the appearance of 'cotton balls'. On the other hand, the 100 nm MFI particles were coated with a much finer layer of $Mg(OH)_2$ and no whisker structure could be seen. X-ray diffraction (XRD) showed that the zeolites maintained the MFI structure (Figure S4). The solvothermally created surface nanostructures were identified as $Mg(OH)_2$ by energy-dispersive spectroscopy (EDS) and XRD (Supporting Information).

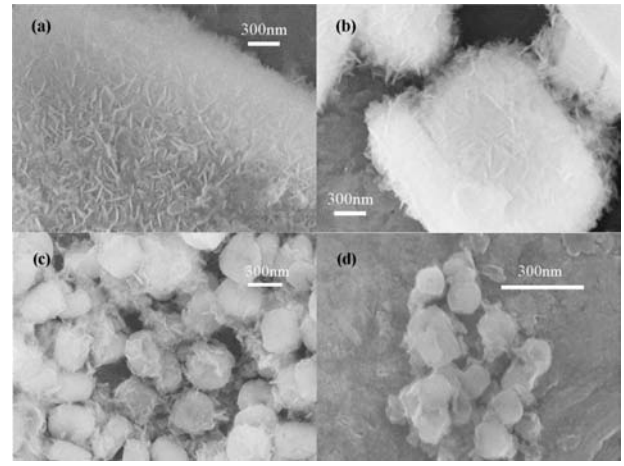

Figure 1. SEM images of solvothermally treated pure-silica-MFI. (a) 5 μm, (b) 2 μm, (c) 300 nm, and (d) 100 nm crystals.

The surface roughness of the MFI crystals was quantified by external surface area measurements, and the results are summarized in Table S3. The surface roughness increased significantly after the surface treatment, and the solvothermally treated MFI crystals showed higher surface areas than Grignard-treated crystals, consistent with our SEM observations of both types of materials (Figures 1 and S2). To examine the effect of solvothermal treatment on the micropore structure (~0.55 nm diameter) of MFI, the micropore volumes of untreated and surface-treated 100 nm MFI crystals were measured by N_2 physisorption. The results were normalized by the mass of MFI (SiO_2) crystals, which is accurately calculated from the overall composition of the surface-treated crystals as obtained by ICP-AES. The micropore volume decreased marginally from 0.15 cm^3/g MFI (untreated) to 0.13 and 0.12 cm^3/g MFI after Grignard or solvothermal treatment, respectively. These results indicate that $Mg(OH)_2$ deposition only marginally affects the porosity of MFI. The ICP-AES measurements also show that at least 96% of the Mg^{2+} in the reactant solution is deposited on the MFI crystal surfaces, thus verifying the high deposition yield.

Figure 2 shows cross sections of mixed matrix membranes made with poly(etherimide) (Ultem, SABIC) and MFI crystals. All membranes made with untreated MFI crystals showed voids at the zeolite/polymer interface. These undesirable "sieve-in-a-cage" morphologies have been reported previously.[2a,8] Smaller MFI crystals also form clusters, resulting in a nonuniform distribution of the molecular sieve. Membranes made with solvothermally modified MFI crystals were uniformly free of interfacial voids and

10.1021/ja907435c CCC: $40.75

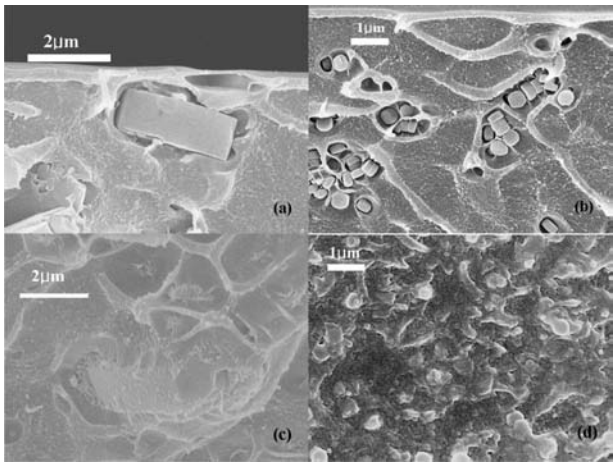

Figure 2. SEM images of cross sections of mixed matrix membranes made with pure-silica-MFI and Ultem. (a) 5 μm untreated MFI, (b) 300 nm untreated MFI, (c) 5 μm solvothermally treated MFI, and (d) 300 nm solvothermally treated MFI.

Table 1. Pure-Component Gas Permeation Properties of Mixed Matrix Membranes Containing 300 nm Solvothermally Treated MFI Crystals at 35°C and 2 atm Upstream Pressure

membrane	CO_2 permeability (Barrer)	CH_4 permeability (Barrer)	CO_2/CH_4 selectivity
pure Ultem[a]	1.4 ± 0.1	0.036 ± 0.001	38 ± 1
20 wt % in Ultem	2.2 ± 0.1	0.051 ± 0.001	43 ± 3
30 wt % in Ultem	2.0 ± 0.1	0.044 ± 0.001	45 ± 2
pure Matrimid[a]	7.6 ± 2.3	0.21 ± 0.07	35 ± 1
35 wt % in Matrimid	31 ± 2	0.78 ± 0.04	39 ± 4

[a] Averaged values from the literature.[3a,9]

demonstrated a highly uniform distribution of MFI crystals in the polymer (especially 300 and 100 nm particles, Figure S8).

Table 1 summarizes pure-component CO_2 and CH_4 gas permeation properties of mixed matrix membranes made with solvothermally modified MFI. High-quality membranes of this type would give large increases in throughput without sacrificing selectivity. Ultem/20 wt % MFI membranes showed a 60% enhancement in CO_2 permeability along with a 15% increase in CO_2/CH_4 selectivity compared to pure Ultem. The use of 30 wt % MFI also showed a higher selectivity and a much higher CO_2 permeability than that of pure Ultem. Matrimid (Vantico)/35 wt % MFI membranes showed a dramatic enhancement in CO_2 permeability and a modest selectivity enhancement over pure Matrimid as well as a substantial selectivity enhancement over membranes made with untreated MFI (Table S4). To show more rigorously that the enhanced gas separation performance is due to the high quality of the polymer/modified-MFI interface, we performed gas permeation measurements with nonporous (uncalcined) MFI crystals, employing O_2 and N_2 as probes. Table 2 shows O_2 and N_2 single-component permeabilities of mixed matrix membranes fabricated with impermeable MFI crystals. In this case, the Maxwell model[1,2a] accurately predicts the permeability of a mixed matrix membrane of the desired ideal morphology (i.e., well-adhered and well-distributed crystals, and no polymer rigidification near the interfaces) without any fitting parameters.

Experimental results from membranes made with solvothermally treated MFI (e.g., Figure 2d) are well matched with the theoretical prediction, indicating excellent adhesion and no significant interfacial polymer rigidification. The latter is also confirmed by DSC

Table 2. Pure-Component Gas Permeation Properties of Ultem and Ultem/MFI Mixed Matrix Membranes at 35°C and 4.5 atm Upstream Pressure (Uncalcined MFI Crystals Used in the Membranes)

membrane	O_2 permeability (Barrer)	N_2 permeability (Barrer)	O_2/N_2 selectivity
pure Ultem	0.43 ± 0.01	0.055 ± 0.002	7.8 ± 0.2
treated MFI/Ultem[a]	0.35 ± 0.01	0.041 ± 0.002	8.5 ± 0.6
treated MFI/Ultem[b] (theoretical prediction)	0.35	0.044	7.8
untreated MFI/Ultem[c]	0.43 ± 0.02	0.056 ± 0.003	7.5 ± 0.7

[a] 20 wt % of solvothermally treated 300 nm MFI in the membrane. [b] Maxwell model; 20 wt % of 300 nm MFI in the membrane.[1,2a] [c] 20 wt % of untreated 300 nm MFI in the membrane.

results (Supporting Information). On the other hand, membranes made with untreated MFI (e.g., Figure 2b) show considerably higher permeability than that of the ideal microstructure, with no positive effect on selectivity. This result is consistent with modified Maxwell model predictions that account for voids at the polymer/zeolite interfaces,[8] but the highly nonideal microstructure of Figure 2b cannot be rigorously described by the model. Our overall results clearly show that the solvothermal deposition process substantially enhances polymer/particle adhesion and is a promising route for processing functional inorganic crystals for membrane applications.

Our method uses an inexpensive inorganic salt as the metal ion source and a recyclable organic solvent. This method can be applied to other surfaces (such as aluminosilicates) and generalized to other hydroxides. We have formed $Mg(OH)_2$ nanostructures on zeolite LTA surfaces. $Ca(OH)_2$ nanostructures were also formed on MFI surfaces, and the functionalized materials showed improved adhesion with Ultem (Figure S11).

Acknowledgment. This work was supported by ExxonMobil Corporation.

Supporting Information Available: Experimental details, SEM images, XRD patterns; EDS, ICP-AES, DSC, and permeation data. This material is available free of charge via the Internet at http://pubs.acs.org.

References

(1) Mahajan, R.; Koros, W. J. *J. Membr. Sci.* **2000**, *175*, 181.
(2) (a) Mahajan, R.; Koros, W. J. *Polym. Eng. Sci.* **2002**, *42*, 1420. (b) Mahajan, R.; Koros, W. J. *Polym. Eng. Sci.* **2002**, *42*, 1432. (c) Pechar, T. W.; Kim, S.; Vaughan, B.; Marand, E.; Tsapatsis, M.; Jeong, H. K.; Cornelius, C. J. *J. Membr. Sci.* **2006**, *277*, 195. (d) Li, Y.; Guan, H.-M.; Chung, T.-S.; Kulprathipanja, S. *J. Membr. Sci.* **2006**, *275*, 17.
(3) (a) Shu, S.; Husain, S.; Koros, W. J. *J. Phys. Chem. C* **2007**, *111*, 652. (b) Shu, S.; Husain, S.; Koros, W. J. *Chem. Mater.* **2007**, *19*, 4000.
(4) (a) Hsu, J. P.; Nacu, A. *Colloids Surf., A* **2005**, *262*, 220. (b) Henrist, C.; Mathieu, J. P.; Vogels, C.; Rulmont, A.; Cloots, R. *J. Cryst. Growth* **2003**, *249*, 321. (c) Lv, J.; Qu, L. Z.; Qu, B. J. *J. Cryst. Growth* **2004**, *267*, 676. (d) Yan, H.; Wu, J. M.; Zhang, X. C.; Zhang, Y.; Wei, L. Q.; Liu, X. G.; Xu, B. S. *J. Mater. Res.* **2007**, *22*, 2544.
(5) (a) Lv, X. T.; Hari, B.; Li, M. G.; Ma, X. K.; Ma, S. S.; Gao, Y.; Tang, L.; Zhao, J. Z.; Guo, Y.; Zhao, X.; Wang, Z. C. *Colloids Surf., A* **2007**, *296*, 97. (b) Yan, C. L.; Xue, D. F.; Zou, L. J.; Yan, X. X.; Wang, W. *J. Cryst. Growth* **2005**, *282*, 448. (c) Yan, L.; Zhuang, J.; Sun, X. M.; Deng, Z. X.; Li, Y. D. *Mater. Chem. Phys.* **2002**, *76*, 119.
(6) (a) Li, Y. D.; Sui, M.; Ding, Y.; Zhang, G. H.; Zhuang, J.; Wang, C. *Adv. Mater.* **2000**, *12*, 818. (b) Ding, Y.; Zhang, G. T.; Wu, H.; Hai, B.; Wang, L. B.; Qian, Y. T. *Chem. Mater.* **2001**, *13*, 435.
(7) Shu, S. PhD Thesis, Georgia Institute of Technology, 2007.
(8) (a) Moore, T. T.; Koros, W. J. *J. Mol. Struct.* **2005**, *739*, 87. (b) Husain, S.; Koros, W. J. *J. Membr. Sci.* **2007**, *288*, 195.
(9) (a) Vu, D. Q.; Koros, W. J.; Miller, S. J. *J. Membr. Sci.* **2003**, *211*, 335. (b) Barbari, T. A.; Koros, W. J.; Paul, D. R. *J. Membr. Sci.* **1989**, *42*, 69. (c) Zhao, H. Y.; Cao, Y. M.; Ding, X. L.; Zhou, M. Q.; Liu, J. H.; Yuan, Q. *J. Membr. Sci.* **2008**, *320*, 179. (d) Zhang, Y.; Balkus, K. J.; Musselman, I. H.; Ferraris, J. P. *J. Membr. Sci.* **2008**, *325*, 28.

JA907435C